NIH Public Access
Author Manuscript
J Immunol. Author manuscript; available in PMC 2013 February 25.

Published in final edited form as:
J Immunol. 2008 May 1; 180(9): 5882–5889.

IFN-γ and IL-17 production in Experimental Autoimmune Encephalomyelitis depends on local APC•T cell complement production*

Jinbo Liu[*], **Feng Lin**[*], **Michael G. Strainic**[*], **Fengqi An**[*], **Robert H. Miller**[†], **Cengiz Z. Altuntas**[‡], **Peter S. Heeger**[§], **Vincent K. Tuohy**[‡], and **M. Edward Medof**[*,1]

[*]Institute of Pathology, Case Western Reserve University

[†]Department of Neurosciences, Case Western Reserve University

[‡]Department of Immunology, Cleveland Clinic, Cleveland, OH, 44106, USA

[§]Department of Medicine, Mt Sinai School of Medicine NY, NY, 10029

Summary

IFN-γ and IL-17 producing T cells autoreactive across myelin components are central to the pathogenesis of multiple sclerosis (MS). Using direct *in vivo*, adoptive transfer, and *in vitro* systems, here we show that the generation of these effectors in $MOG_{35–55}$ induced EAE depends on interactions of locally produced C3a/C5a with APC and T cell C3aR/C5aR. In the absence of the cell surface C3/C5 convertase inhibitor decay accelerating factor (DAF) but not the combined absence of DAF and C5aR and/or C3aR on APC and T cells, a heightened local autoimmune response occurs in which myelin destruction is markedly augmented in concert with markedly more IFN-γ+ and IL-17^+ T cell generation. The augmented T cell response is due to increased IL-12 and IL-23 elaboration by APCs together with increased T cell expression of the receptors for each cytokine. The results apply to initial generation of the IL-17 phenotype since naïve $CD62L^{hi}$ *Daf1*$^{-/-}$ T cells produce 3-fold more IL-17 in response to TGF-β and IL-6 while $CD62L^{hi}$ *Daf1*$^{-/-}$*C5aR*$^{-/-}$*C3aR*$^{-/-}$ T cells produce 4-fold less.

Keywords

Decay Accelerating Factor; EAE; T cell; Autoimmunity; Epitope spreading

Introduction

Experimental autoimmune encephalomyelitis [EAE (1)] is a rodent model that has been valuable for characterizing immunopathogenic processes that underlie multiple sclerosis (MS). One way that disease is induced is adjuvant and pertussis toxin boosted immunization of C57BL/6 mice with the encephalitogenic peptide (p35–55) of myelin oligodendrocyte glycoprotein (MOG), an external myelin component. Following this immunization, myelin sheaths of oligodendrocytes are attacked (2).

[*]The work was supported by National Institute of Health, MEM (AI23598 and EY-11288), VKT (AI-51837 and DC-006422), FL (RG3664-A-1 and NS052471), RHM (N536674), and E. Pearlman (core facility EY015476).

[1]Address correspondence to: M. Edward Medof, M.D., Ph.D., Institute of Pathology, Case Western Reserve University, School of Medicine, 2085 Adelbert Road, Room 301, Cleveland, Ohio 44106, (216) 368-5434, fax: (216) 368-0495, mxm16@case.edu.

NIH-PA Author Manuscript
NIH-PA Author Manuscript
NIH-PA Author Manuscript

NIH-PA Author Manuscript

NIH-PA Author Manuscript

NIH-PA Author Manuscript

According to current concepts (3), myelin destruction in EAE (and MS) is caused by T cells autoreactive with myelin which are peripherally activated, and upon encountering microglia bearing myelin peptides in the brain become further activated (4). A feature of EAE pathogenesis that closely relates to MS pathogenesis is that autoreactivity induced against the myelin immunogen, e.g. MOG, broadens to other myelin components, e.g. proteolipid protein (PLP) and myelin basic protein (MBP). This process termed “epitope spreading” is thought to be due to endogenous priming to new self determinants during initial and subsequent inflammatory interactions (5). For reproducing it, rather than the C57BL/6 H-2^b strain, the autoreactive-prone SJL H-2^s strain generally is used.

In previous studies (6), we found that decay accelerating factor (DAF or CD55), a regulator originally characterized as a plasma membrane shield that circumvents C3b deposition on self cell surfaces and prevents C5 activation (7), modulates T cell responses (see Discussion). In its absence on APCs or on cognate $CD4^+$ and $CD8^+$ T cells interacting with them, proliferative and IFN-γ responses are 5–22 fold augmented. Findings that double deficiency of DAF and factor D (fD), an alternative pathway component, abolished the enhancement *in vitro* as well *in viv*o linked the effect to complement locally produced by APC•T cell partners. Prompted by this result, we analyzed flow sorted WT APCs and T cells following mixing with specific peptide and found that early during cognate interactions both partners locally synthesize all three alternative pathway components i.e. C3, factor B (fB), and fD together with C5 as well as C5a and C3a receptors (C5aR and C3aR). We found that concomitant with this local complement synthesis, both APCs and T cells downregulate surface DAF expression lifting restraint on junctional activation. We further found that C5a and C3a are locally generated by both partners and that the interaction of these activation fragments with C5aR and C3aR on both partners promotes both APC and T cell cytokine production (8). While other investigators have reported that autoimmune diseases are diminished in the absence of C5aR or C3aR and attributed the findings to effects of serum complement (9–11), our findings that a) APC and T cells locally synthesize complement b) DAF restraint on junctional activation is lifted in concert with the local complement synthesis and c) that interactions of locally generated C5a and C3a with C5aR and C3aR promotes cytokine production, prompted us to investigate whether interaction of locally produced C5a and C3a with C5aR and C3aR on APCs and T cells impacts autoimmunity and, if so, how.

In the present investigation, we exploited Daf deficient mice in the $MOG_{35–55}$-induced EAE model to study a) the extent to which DAF influences T cell autoreactivity to self antigens, b) whether its presence is necessary to protect against broadening of the anti-myelin T cell response, c) the nature of the T cell response elicited in its absence, and d) the mechanism of the any observed differences.

Materials and Methods

Animals

Eight to 12 week old female *Daf1*$^{-/-}$ mice (12) and their *Daf1*$^{+/+}$ female littermates backcrossed 5 generations on the C57BL/6 background were used. Although mice possess a second *Daf* gene [*Daf2* (13)], which encodes transmembrane-anchored Daf expressed almost exclusively in the testes. Studies were carried out using an approved Institutional Animal Care and Use Center (IACUC) protocol.

Antigens

Rat $MOG_{35–55}$ MEVGWYRSPFSRVVHLYRNGK, the immunodominant encephalitogen for C57BL/6 mice (14) was synthesized using standard solid phase methodology and 9-

NIH-PA Author Manuscript

NIH-PA Author Manuscript

NIH-PA Author Manuscript

fluorenylmethoxycarbonyl (FMOC) side chain protected amino acids, purified >90% by reverse phase HPLC, and confirmed by mass spectrometry. PLP was purified from a washed total lipid extract of human white matter and converted to aqueous form as described (15). Mouse MBP was purchased from Sigma (St. Louis, MO). Mouse IL-4 and GM-CSF were purchased from Peprotech (Rockyhill, NJ). Anti-CD3, anti-CD28, anti-IFN-γ and anti-IL-4 monoclonal antibodies (mAbs) were purchased from BD Pharmingen (San Diego, CA).

Induction and Evaluation of EAE

Animals were injected sc with 100 μg of $MOG_{33–35}$ in CFA containing 400 μg of mycobacterium tuberculosis H37RA (Difco, Detroit, MI). Upon immunization and two days later, 200 ng of pertussis toxin (List Biological Labs Inc., Campbell, CA) was injected ip. Mice were weighed and scored for neurological deficits daily: 0=no disease; 1=decreased tail tone or slightly clumsy gait; 2=tail atony; 3=limb weakness; 4=limb paralysis; 5=moribund state.

Adoptive transfer of T cells

18 days after priming 8–12 wk old female *Daf1*$^{-/-}$ or *Daf1*$^{+/+}$ mice with $MOG_{35–55}$ in CFA containing H37RA, splenocytes were cultured for 72 hr with 20 μg/ml of $MOG_{35–55}$ and 10 ng/ml of IL-12 or IL-23. In initial studies (3×10^7) washed cells from *Daf1*$^{-/-}$ mice or *Daf1*$^{+/+}$ mice were administered ip into *Daf1*$^{+/+}$ recipients that received 400 rads of γ irradiation. Guided by 4 or 3-fold higher numbers of IFN-γ or IL-17 producing cells, in subsequent studies, washed spleen cells (40 or 30×10^6) from *Daf1*$^{+/+}$ mice vs 10×10^6 from *Daf1*$^{-/-}$ mice were transferred to obtain equal numbers of IFN-γ or IL-17 producing cells. Clinical scores and weights were monitored as above.

Histology and Myelin Staining

Spinal cords were collected at days 18 and 56 from 4–8 mice in each group, fixed after infusion with 100 ml of 4% paraformaldehyde for 5 min, embedded in OCT, quick frozen in liquid N_2 and stored at −70°C. Cryostat sections (10–20 μm) were evaluated at ten levels. H&E staining was done by standard methods. Alcohol-dehydrated sections were stained for myelin in Luxol Fast Blue (Sigma Inc., St. Louis MO) overnight at 37°C and agitated for 10 sec in 0.0005% lithium carbonate and 60 sec in 70% alcohol.

Electron Microscopy (EM)

Spinal cords were fixed in formaldehyde/glutaraldehyde (3%)/0.1 M sodium cacodylate, post-fixed in 1% osmium tetroxide and embedded in LX112 resin (Polysciences Inc., PA). Ultrathin uranyl acetate/lead citrate-stained sections were cut and examined with a JEOL 100cx microscope.

Proliferation and ELISPOT Assays

Splenocytes (2×10^5 cells in 200 μl) were cultured for 96 hr in triplicate in 96-well microtiter flat bottom plates with 0.01–100 μg/ml of $MOG_{35–55}$, pulsed for 16 hr with [*methyl*-^{3}H] thymidine (1 μCi/well; sp. act., 6.7 Ci/mmol; New England Biolabs, Boston, MA) and incorporated radioactivity expressed as the mean cpm of triplicate Ag containing wells. In ELISPOT assays, splenocytes ($2–6 \times 10^5$) were incubated for 24 hr in anti-IFN-γ or IL-17 mAb (R&D System, Minneapolis, MN) coated and PBS-1% BSA blocked 96 well ELISPOT plates (Whatman, Clifton, NJ) with 0.01–20 μg/ml of MOG 35–55, 0.01–50 μg/ml of PLP or 100 μg/ml of MBP and spots were developed and quantitated on an ELISPOT analyzer (Cellular Technology Ltd., Cleveland, OH).

NIH-PA Author Manuscript

NIH-PA Author Manuscript

NIH-PA Author Manuscript

Murine DCs

Bone marrow cells from mice were grown in RPMI 1640 (containing 10% FBS, 10 μg/ml IL-4 and 10 μg/ml GM-CSF). The medium was changed on day 3 and day 5. Cells were used on Day 6.

RNA purification, cDNA synthesis and qPCR

Total RNA was purified by Qiagen RNeasy mini kit (Qiagen Inc, La Jolla, CA). cDNA was synthesized from 20 μl of mRNA in Sprint PowerScript Single Shots (Clontech, Mountain View, CA). Diluted cDNA (10 μl) was mixed with 2 μl of primer and 10 μl SYBR green master mix (Applied Biosystems, Foster City, CA). Each sample was assayed in duplicate on an ABI prism 7000 cycler. In all assays, fold-increases are relative to basal levels and standardized to Actin.

Western Blotting

All blots were performed as previously described (16) using HRP-conjugated secondary antibody, and an ECL enhancer (GE Healthcare, Buckinghamshire, UK).

Induction of IL-17 with IL-6 and TGF-β

Lymph node cells were harvested from 5 *Daf1*$^{+/+}$, 5 *Daf1*$^{-/-}$, and 5 *Daf1*$^{-/-}$*C5aR*$^{-/-}$*C3aR*$^{-/-}$ mice and naïve CD4 +CD62L^{hi} cells were sorted. The sorted (CD4^{+}CD62L^{hi}) T cells were stimulated with anti-CD3 (5 μg/ml), anti-CD28 (10 μg/ml), anti-IFN-γ (10 μg/ml), anti-IL-4 (10 μg/ml) antibodies together with TGF-β (20 ng/ml) or TGF-β plus IL-6 (20 ng/ml). IL-17 production in culture supernatants was measured by the Beadlyte Mouse 21-plex Cytokine Detection System (Upstate, CA) after 72 hr of activation.

Statistics

A repeated measures cumulative logit model (17), using the equation, $\log it[P(Y \le j \mid x)] = \alpha_j + \beta_1 genotype + \beta_2 time + \beta_3 genotype * time$, was used to test for the differences in groups across time points, with α_j corresponding to the P (Y ≤ j) for each threshold or score and β corresponding to the coefficients to be estimated for the main effects of genotype and time as well as for the interaction between genotype and time. Calculations were performed on SAS for Windows 9.1. Statistics for the *in vitro* studies were done by Student's *t*-test.

Results

Severity of EAE is increased in *Daf1*$^{-/-}$ mice

To determine how DAF deficiency influences CNS neuronal injury in EAE, we immunized 12 *Daf1*$^{-/-}$ mice and 12 *Daf1*$^{+/+}$ littermates with $MOG_{35–55}$ and monitored them daily. While all mice in both groups developed EAE, neurologic dysfunction in *Daf1*$^{-/-}$ mice was markedly more severe. Fig. 1A shows clinical scores over a 62 day period from the above mice combined with 12 more *Daf1*$^{-/-}$ and *Daf1*$^{+/+}$ mice from an identical repeat experiment (total of 24 mice in each group). In the *Daf1*$^{-/-}$ mice, the mean clinical score was 3.5 ± 1.1 vs. 1.7 ± 1.3 in *Daf1*$^{+/+}$ littermates ($p < 0.001$), and the mean weight decrease (over days 10 to 62) was greater (91.2±2.8% of original weight vs 97.8±3.4%, $p < 0.05$) (not shown). While by day 40 onward most *Daf1*$^{+/+}$ mice exhibited only minimal physical changes, some *Daf1*$^{-/-}$ mice had to be euthanized because they barely moved.

Heightened disease severity in *Daf1*$^{-/-}$ mice is due to heightened cellular autoreactivity

To document that the heightened disease severity in *Daf1*$^{-/-}$ mice was mediated by increased cellular immunity (since DAF also inhibits cytotoxicity conferred by systemic

NIH-PA Author Manuscript

NIH-PA Author Manuscript

NIH-PA Author Manuscript

complement), we performed adoptive transfer experiments in which we injected equal numbers of splenocytes from $MOG_{35–55}$-immunized *Daf1*$^{-/-}$ or *Daf1*$^{+/+}$ mice into naïve *Daf1*$^{+/+}$ recipients. As seen in Fig 1B, compared to *Daf1*$^{+/+}$ recipients that received *Daf1*$^{+/+}$ splenocytes, *Daf1*$^{+/+}$ recipients that received *Daf1*$^{-/-}$ splenocytes showed ≥ 2 fold higher clinical scores and more profound weight decreases (data not shown). The difference in disease severity was comparable to that following direct immunization with $MOG_{35–55}$.

In contrast to the enhancement of T cell responses in *Daf1*$^{-/-}$ mice, assays of day 56 sera showed that both groups elaborated similar amounts of anti-MOG antibodies. Moreover, *Daf1*$^{-/-}$ mice did not generate more complement fixing IgG2a, IgG2b, or IgM (not shown). Staining of [perfused (see Methods)] spinal cords (day 56) for deposited C3 and C9 showed that while some deposition of both components was detectable in *Daf1*$^{-/-}$ mice and *Daf1*$^{+/+}$ littermates, pixel counts showed no significant differences [650 ± 123 vs 530 ± 120 for C3 ($p > 0.05$) and 630 ± 194 vs 570 ± 121 for C9 ($p > 0.05$) (data not shown)].

Daf1 $^{-/-}$ mice suffer greater CNS leukocyte infiltration and demyelination and myelin does not recover

To compare pathology, we examined dorsal columns of *Daf1*$^{-/-}$ and *Daf1*$^{+/+}$ mice at early (day 18) and late (day 56) disease stages. At the day 18 time point, H&E staining showed markedly increased leukocyte infiltration in *Daf1*$^{-/-}$ mice which on high power examination were >90% lymphocytes and macrophages (Fig. 2 A,B). Luxol Fast Blue staining at both day 18 and 56 showed markedly more myelin loss in *Daf1*$^{-/-}$ mice (Fig. 2 C,D). Ultrastructural analyses at both the early and late time points confirmed markedly increased destruction of myelin sheaths (not shown). Moreover, while at late stages of disease (day 84), *Daf1*$^{+/+}$ mice demonstrated remyelination [as indicated by small thinly myelinated axons in lesional areas (Fig. 2 E)], little, if any, remyelination was detectable in the *Daf1*$^{-/-}$ mice (Fig. 2F).

Greater disease severity in *Daf1* $^{-/-}$ mice is due to the augmented generation of IFN-γ and IL-17 producing cells

To determine the immunological basis for the heightened disease in *Daf1*$^{-/-}$ mice, we measured T cell responses to $MOG_{35–55}$ peptide. In [^{3}H]-thymidine incorporation assays (not shown) at day 28 postimmunization, *Daf1*$^{-/-}$ splenic T cells expanded 5-fold more than *Daf1*$^{+/+}$ spleen cells (2000 vs 400 cpm/10^5 spleen cells at 1μg/ml $MOG_{35–55}$). IFN-γ and IL-17 ELISPOT assays at 30 days showed 5–6 fold more IFN-γ producing cells and 2-fold more IL-17 producing cells than in *Daf1*$^{+/+}$ spleens (Fig. 3). Later in disease (60 days), these assays showed 4–5-fold more IFN-γ producing cells and 5–7-fold more IL-17 producing cells than in *Daf1*$^{+/+}$ spleens. At an even later time point (75 days) the ELISPOT assays showed that the ratio of IL-17 producing cells to IFN-γ producing cells in *Daf1*$^{+/+}$ mice declined to 2:1, while the ratio of IL-17 producing cells to IFN-γ producing cells in *Daf1*$^{-/-}$ mice remained more than 6:1 indicating that the IL-17 response in *Daf1*$^{-/-}$ mice is more sustained. ELISAs of supernatants of spleen cells from *Daf1*$^{-/-}$ and *Daf1*$^{+/+}$ mice at day 56 showed increases in IL-2, IFN-γ, and IL-17, and decreases in IL-5 and IL-10 in the *Daf1*$^{-/-}$ mice, consistent with augmented Th1 and Th17 responses (data not shown). IFN-γ and IL-17 ELISAs of cultured spleen supernatants at day 56 verified 3–4 fold elevated levels of IFN-γ and 5–6 fold elevated levels of IL-17 (not shown). Computer analyses of mean ELISPOT sizes showed similar IL-17 spot sizes but larger IFN-γ spot sizes (Fig 3C). Repeat adoptive transfer experiments this time adjusting spleen cells for equal numbers of IFN-γ or IL-17 producing cells showed that, even under these conditions, *Daf1*$^{-/-}$ spleen cells in each case conferred greater pathology (Fig 3D).

NIH-PA Author Manuscript

NIH-PA Author Manuscript

NIH-PA Author Manuscript

The T cell response in *Daf1*$^{-/-}$ mice shows intermolecular epitope spreading

To determine whether the enhanced immunoreactivity in *Daf1*$^{-/-}$ mice was sufficient to overcome the normal resistance in H-2^{b} mice to epitope spreading (5), we performed IFN-γ ELISPOT recall assays at days 13–64 with PLP and MBP. Consistent with past literature (18), no PLP reactivity was observed with spleen cells from *Daf1*$^{+/+}$ controls (Fig. 4A). In contrast, dose-dependent PLP reactivity (Fig 4A) developed between day 56 and 64 (Fig. 4B) in *Daf1*$^{-/-}$ mice. As with PLP, *Daf1*$^{-/-}$ spleen cells also showed reactivity to MBP (Fig. 4C). Reactivity to neither PLP nor MBP was detectable in spleens of unprimed *Daf1*$^{-/-}$ mice, verifying that the elicited autoreactives were dependent upon MOG immunization.

The heightened IFN-γ and IL-17 production by *Daf1*$^{-/-}$ T cells is dependent on amplified interactions of C3a and C5a with APC C3aR and C5aR resulting in increased IL-12 and IL-23 production

Our previous studies (6) showed that when APCs and cognate T cells interact, both partners turn on the local synthesis of complement and concomitantly downregulate DAF. Because a) DAF regulates C3/C5 convertases (7), b) prior reports have suggested that the anaphylatoxin receptors C3aR and C5aR can be involved in T cell mediated disease models (9, 10), and c) we showed that exogenous C5a augments alloreactive T cell immunity (6), we tested whether increased local C5a/C3a•C5aR/C3aR interaction by *Daf1*$^{-/-}$ APCs and T cells can account for the greater anti-MOG autoreactive response in *Daf1*$^{-/-}$ mice as well as explain previous findings by others with *C5aR*$^{-/-}$ and *C3aR*$^{-/-}$ mice attributed to “crosstalk” from serum complement.

To determine whether increased local C5a/C3a•C5aR/C3aR interaction by *Daf1*$^{-/-}$ APCs and T cells is involved in the increased IFN-γ and IL-17 production in *Daf1*$^{-/-}$ mice and, if so, how the two processes are mechanistically linked. We performed two sets of *in vitro* studies. In one, we stimulated transgenic OT-II T cells with *Daf1*$^{+/+}$, *Daf1*$^{-/-}$, and *Daf1*$^{-/-}$ *C3aR*$^{-/-}$ *C5aR*$^{-/-}$ dendritic cells (DCs) in the presence of specific ova$_{323–339}$ peptide and examined the production of IL-12 and IL-23 by the DCs. In the other, we stimulated *Daf1*$^{+/+}$, *Daf1*$^{-/-}$, *Daf1*$^{-/-}$ *C3aR*$^{-/-}$, and *Daf1*$^{-/-}$ *C5aR*$^{-/-}$ T cells with anti-CD3 and anti-CD28 mAbs and assessed the effects of IL-12 or IL-23 addition on T cell IFN-γ and IL-17 production. The two sets of studies showed that a) *Daf1*$^{-/-}$ DCs produced 4-fold more IL-12 and 5-fold more IL-23 than *Daf1*$^{+/+}$ DCs (Fig 5A), b) the addition of IL-12 to anti-CD3/CD28 stimulated *Daf1*$^{-/-}$ T cells produced 4-fold more IFN-γ producing cells and the addition of IL-23 produced 5-fold more IL-17 producing cells compared to *Daf1*$^{+/+}$ controls (Fig 5B), c) the heightened responses of *Daf1*$^{-/-}$ T cells were associated with upregulation of their IL-12Rβ2 and IL-23R levels (Fig 5C), and d) the augmented IFN-γ and IL-17 production by *Daf1*$^{-/-}$ T cells depended on T cell C3aR and C5aR (Figs 5B and 6C).

In support of the dependence of the augmented IFN-γ and IL-17 responses on C5aR and C3aR on both APCs and T cells, a) the increased production of IL-12 and IL-23 by *Daf1*$^{-/-}$ APCs was abrogated in *Daf1*$^{-/-}$ *C3aR*$^{-/-}$ *C5aR*$^{-/-}$ triple knockout APCs (Fig 6A), b) western blots of supernatants of anti-CD3/CD28 stimulated *Daf1*$^{+/+}$, *Daf1*$^{-/-}$, *Daf1*$^{-/-}$ *C3aR*$^{-/-}$, and *Daf1*$^{-/-}$ *C5aR*$^{-/-}$ T cells showed that *Daf1*$^{-/-}$ cells but not *Daf1*$^{-/-}$ *C3aR*$^{-/-}$ or *Daf1*$^{-/-}$ *C5aR*$^{-/-}$ cells produced more C3a and C5a (the ligands for C3aR and C5aR) than *Daf1*$^{+/+}$ cells (Fig 6B), c) the increased IFN-γ and IL-17 responsiveness of *Daf1*$^{-/-}$ T cells to IL-12 and IL-23 was abrogated in *Daf1*$^{-/-}$*C5aR*$^{-/-}$ and *Daf1*$^{-/-}$*C3aR*$^{-/-}$ mice (Fig 5B), d) ELISPOT assays showed that the increased numbers of IFN-γ and IL-17 producing cells generated by anti-CD3/CD28 stimulated *Daf1*$^{-/-}$ T cells were abolished with *Daf1*$^{-/-}$*C5aR*$^{-/-}$ and *Daf1*$^{-/-}$*C3aR*$^{-/-}$ T cells (Fig 6C), and e) ELISAs showed that the augmented IFN-γ and IL-17 also depended C3 and fD (Fig 6D).

NIH-PA Author Manuscript

NIH-PA Author Manuscript

NIH-PA Author Manuscript

Daf1$^{-/-}$ T cells produce more IL-17 in response to TGF-β and IL-6

Recent studies (19) of sorted naïve CD4^{+} CD62L^{hi} cells have shown that IL-17 producing cells are not generated directly from IL-23 stimulation but rather are initially induced by IL-6 and TGF-β. Once differentiated by these cytokines, IL-23 augments and sustains IL-17 production. To ascertain how the results in this study relate to this finding, we flow sorted *Daf1*$^{+/+}$ and *Daf1*$^{-/-}$ CD4^{+} CD62L^{hi} cells and incubated the sorted cells with anti-CD3+anti-CD28 mAbs for 72 hr in the presence of IL-6 and TGF-β together with anti-IFN-γ and anti-IL-4 mAbs, exactly as described in the above published study (19). An ELISA of supernatants (Fig 7A) of the treated cells showed three times more IL-17 production by naïve *Daf1*$^{-/-}$ T cells than by naïve *Daf1*$^{+/+}$ cells. Compared to WT T cells, IL-17 production was reduced 4-fold when *Daf1*$^{-/-}$*C3aR*$^{-/-}$*C5aR*$^{-/-}$ cells were used.

The dependence of T cell IFN-γ and IL-17 production on C5a/C3a•C5aR/C3aR interactions applies *in vivo*

To document that the above *in vitro* linkage of C5a/C3a•C5aR/C3aR interactions with T cell IFN-γ and IL-17 production applies *in vivo* and correlates with EAE disease severity, we compared clinical scores in *Daf1*$^{-/-}$, *Daf1*$^{-/-}$ *C5aR*$^{-/-}$, *Daf1*$^{-/-}$ *C3aR*$^{-/-}$, and *Daf1*$^{+/+}$ mice following immunization with MOG$_{35–55}$. Consistent with the *in vitro* data in Fig 6A–D, the increased disease severity in *Daf1*$^{-/-}$ mice over that in *Daf1*$^{+/+}$ mice was not only abrogated in *Daf1*$^{-/-}$ *C5aR*$^{-/-}$ and *Daf1*$^{-/-}$ *C3aR*$^{-/-}$ mice, but clinical scores went below those of *Daf1*$^{+/+}$ mice (Fig 7B).

Taken together, the data indicate that heightened disease activity in *Daf1*$^{-/-}$ mice is due to 1) heightened production of IL-12/IL-23 by *Daf1*$^{-/-}$ APCs and 2) heightened IFN-γ and IL-17 responses by *Daf1*$^{-/-}$ T cells to the two APC "signal 3" cytokines resulting (at least in part) from higher induced levels of IL-12β2R and IL-23R. The studies with *Daf1*$^{-/-}$ cells doubly deficient in C5aR or C3aR show that a) the augmented cytokine production by both partners depends on APC•T cell C5a/C3a•C5aR/C3aR interactions and b) the dependence on these interactions applies *in vivo* in that they control EAE disease severity.

Discussion

The results of this study document an important role for DAF function in shielding against T cell autoreactivity. T cell autoimmunity in *Daf1*$^{-/-}$ mice immunized with MOG$_{35–55}$ is stronger; EAE is more severe; more T cells are present in the CNS; myelin loss is more extensive; and remyelination is impaired. That the heightened CNS injury is, in fact, mediated by augmented T cell reactivity was formally established by adoptive transfer. The autoreactive response is both quantitatively and qualitatively different in that it is not only associated with more IFN-γ producing cells but even more IL-17 producing cells. As assessed by both proliferation and by IFN-γ and IL-17 ELISPOT assays, the increased lymphocyte infiltration in *Daf1*$^{-/-}$ mice is due to up to a 5-fold more robust T cell IFN-γ response and 7-fold more robust T cell IL-17 response to the priming by MOG immunogen. When equalized for IFN-γ producing cells or IL-17 producing cell numbers, adoptively transferred spleen cells induce greater disease severity. As a result, despite the inherent resistance of the H-2^{b} background to epitope spreading, the enhanced autoreactivity allows intermolecular spreading to PLP and MBP. Taken together, the findings argue that DAF serves as a barrier to the induction of T cell autoreactivity in EAE and that its protection is conferred via inhibition of the induced T cell autoreactivity to myelin and spreading of the autoreactivity to other myelin components.

Until this report, significant epitope spreading has been observed primarily in SJL/J or SWXJ mice and has not been extensively described in C57BL/6 H-2^{b} mice. Our findings of

NIH-PA Author Manuscript

NIH-PA Author Manuscript

NIH-PA Author Manuscript

markedly stronger T cell responses in C57BL/6 H-2^b *Daf1*$^{-/-}$ mice and spreading of autoreactivity to PLP and MBP are consistent with the observed augmented myelin destruction. To our knowledge, the finding that T cell reactivity to PLP and MBP is induced by $MOG_{35–55}$ in the absence of DAF, i.e. that the barrier to extension of T cell reactivity to myelin components other than the $MOG_{35–55}$ immunogen is overcome, constitutes the first definitive demonstration of H-2^b-restricted intermolecular epitope spreading.

The adoptive transfer experiments (Fig 1C) showed that the enhanced disease was directly related to *Daf1*$^{-/-}$ donor cells. Thus, priming to self in a DAF-deficient milieu produces an uncontrolled hyper-autoreactivity that leads to severe disease sequelae. Although it is clear that DAF serves as a global negative regulator of T cell activation, the overall permissive impact of DAF deficiency in EAE severity is the overrepresentation of the Th17 as well as the Th1 lineage. While the association is not causally proven in this study, the linkage of severe EAE outcome to increased frequencies of IL-17 producing T cells is consistent with many recent studies showing a) greater autoimmune severity following transfer of such Th17 T cells, b) amelioration of disease following IL-17 neutralization in WT mice, and c) reduced EAE susceptibility in *IL17*$^{-/-}$ mice (20–23). It is possible that DAF expression may tip this fine balance away from IFN-γ and Th-17 mediated enhanced disease and that unregulated local complement production by APCs, T cells, or both may shape the autoimmune repertoire by allowing excessive selection of the IFN-γ and Th17 lineages. In support of this, in addition to the number of anti-$MOG_{35–55}$ IL-17 producing cells being greater in the *Daf1*$^{-/-}$ mice, the rate of decline in the number of these cells was slower than in *Daf1*$^{+/+}$ mice possibly accounting for the absence in these mice of myelin repair. Thus, DAF may serve overall to prevent or limit severe autoimmune outcomes due to IFN-γ and particularly to Th17 mediated events.

Our studies with *Daf1*$^{-/-}$ DCs and T cells doubly deficient in *C5aR*$^{-/-}$*C3aR*$^{-/-}$ or *C3*$^{-/-}$ relate the mechanism underlying DAF's T cell immunomodulatory activity to our newly uncovered findings (6) that an early event (<1 hr) during APC•T cell cognate interactions is that both partners turn on local synthesis of C3, fB, fD (the three alternative pathway components) and downregulate DAF. More recent work[1] has shown that both cognate partners additionally synthesize C5, upregulate C5aR and C3aR, and in the context of diminished junctional DAF, generate C5a and C3a from the locally synthesized components. This recent work has shown that interactions of these locally generated anaphylatoxins with upregulated C5aR and C3aR in both partners augments costimulation. The *in vitro* experiments in this study with *Daf1*$^{-/-}$, *Daf1*$^{+/+}$ and doubly deficient *Daf1*$^{-/-}$*C5aR*$^{-/-}$ or doubly deficient DCs and T cells shows that the augmented IFN-γ and IL-17 production in *Daf1*$^{-/-}$ mice is due both to a) more IL-12 and IL-23 production by *Daf1*$^{-/-}$ DCs than WT DCs, b) upregulated expression of IL-12Rβ2 and IL-23R on *Daf1*$^{-/-}$ T cells, and c) increased production of IFN-γ and IL-17 of *Daf1*$^{-/-}$ T cells in response to IL-12 and IL-23, respectively. The western blot analyses of culture supernatants showing increased C5a and C3a production by *Daf1*$^{-/-}$ T cells and the ELISPOT assays and ELISAs showing reversal of the heightened IFN-γ and IL-17 production when *Daf1*$^{-/-}$*C5aR*$^{-/-}$ or *Daf1*$^{-/-}$*C3aR*$^{-/-}$ T cells were used document that the T cell autoreactivity is dependent on local C5a/C3a generation and consequent C5aR/C3aR signaling. While the work in this study was done with Daf deficient cells, our previous findings in WT cells (6) that in concert with local complement/C5aR/C3aR synthesis, DAF downregulates on both APCs and T cells establish that *Daf1*$^{-/-}$ T cells simulate activation events in normal cells. Since the heightened reactivity of T cells occurs in the absence of DAF on APCs (6) and T cells[2], this newly

[1]Strainic et. al., submitted and Lalli, et. al., submitted)
[2]Strainic et. al., submitted and Lalli, et. al., submitted)

NIH-PA Author Manuscript

NIH-PA Author Manuscript

NIH-PA Author Manuscript

uncovered process is not related to older studies (24, 25) putatively linking DAF to direct signaling *per se*.

Our studies with naïve $CD4^+$ $CD62L^{hi}$ cells relate our results to recent findings (26) that differentiation of naïve T cells into the Th17 lineage is dependent on TGF-β and IL-6. It has been shown that TGF-β mediates upregulation of IL-23 receptors on T cells (19, 27–31). Our incubations of sorted $CD4^+$ $CD62L^{hi}$ naïve *Daf1*$^{-/-}$ and *Daf1*$^{+/+}$ T cells with TGF-β and IL-6 showed that *Daf1*$^{-/-}$ T cells produce 3-fold more IL-17. Our studies with *Daf1*$^{-/-}$*C5aR*$^{-/-}$*C3aR*$^{-/-}$ cells showed that the increases depended on C5aR/C3aR function. More work is needed to determine the source of these cytokines and whether local complement synthesis is involved in their production.

Humoral immunity against myelin has been implicated in EAE, but its involvement generally relates to induction of disease with whole protein rather than peptide (32). When immunized with whole MOG protein, B cell-deficient mice develop less severe EAE (32). In contrast, if $MOG_{35–55}$ is used, demyelination in the B cell knockouts is similar to that in WTs (33). The experiments in this study showing no significant difference in complement-fixing Igs or C3/C9 deposition, document that DAF's activity on T cells is distinct from DAF's traditional self cell-shielding role against systemic complement-mediated injury. Lower clinical scores in *C3*$^{-/-}$ mice (34) and in *C3aR*$^{-/-}$ mice (11) are consistent with the results in this study concerning locally generated complement activation fragments enhancing activation during T cell priming (6). Whether the findings in this study that DAF participates in protecting myelin from autoreactive T cells in EAE is a general phenomenon for autoimmunity and T cell reactivity in other contexts must await further work. Results available so far with corneal transplantation (35) would support this possibility.

In MS, like EAE, MOG is a target autoantigen (36). As in EAE, MHC class II restricted T cells reactive with MOG are present in MS patients' cerebrospinal fluid (37). Currently, acute attacks are treated with intravenous steroids, IFN-β, Copaxone, and immunosuppressives, but overall, available treatments are unsatisfactory (38). Our findings that markedly enhanced EAE occurs in *Daf1*$^{-/-}$ mice due to lowering the threshold to T cell autoreactivity raise the possibility that appropriately targeted recombinant DAF could have therapeutic relevance for MS.

Acknowledgments

The authors thank Dr. BP Morgan, Cardiff, UK, for rabbit anti-rat C9, Dr. Mireya Diaz-Insua (Dept of Statistics, CWRU) for statistical analyses, and Denny Hatala for preparing tissue sections.

Abbreviations used in this paper

MS	multiple sclerosis
EAE	experimental autoimmune encephalomyelitis
BBB	blood brain barrier
MOG	myelin oligodendrocyte glycoprotein
CNS	central nervous system;
MBP	myelin basic protein
PLP	proteolipid protein
DAF	decay accelerating factor

NIH-PA Author Manuscript

NIH-PA Author Manuscript

NIH-PA Author Manuscript

daf1	mouse homolog of human DAF protein
C5aR and C3aR	C5a receptor and C3a receptor

References

1. Gold R, Hartung HP, Toyka K. Animal models for autoimmune demyelinating disorders of the nervous system. Mol Med Today. 2000; 6:88–88. [PubMed: 10652482]
2. Merkler D, Oertle T, Buss A, Pinschewer DD, Schnell L, Bareyre FM, Kerschensteiner M, Buddeberg BS, Schwab M. Rapid induction of autoantibodies against Nogo-A and MOG in the absence of an encephalitogenic T cell response: implication for immunotherapeutic approaches in neurological diseases. FASEB Journal. 2003; 17:2275–2275. [PubMed: 14563689]
3. Kohm AP, Miller SD. Role of ICAM-1 and P-selectin expression in the development and effector function of CD4+CD25+regulatory T cells. J Autoimmun. 2003; 21:261–271. [PubMed: 14599851]
4. Linnington C, Berger T, Perry L, Weerth S, Hinze-Selch D, Zhang Y, Lu HC, Lassmann H, Wekerle H. T cells specific for the myelin oligodendrocyte glycoprotein mediate an unusual autoimmune inflammatory response in the central nervous system. Eur J Immunol. 1993; 23:1364–1364. [PubMed: 7684687]
5. Tuohy VK, Yu M, Yin L, Kawczak JA, Johnson JM, Mathisen PM, Weinstock-Guttman B, Kinkel RP. The epitope spreading cascade during progression of experimental autoimmune encephalomyelitis and multiple sclerosis. Immunol Rev. 1998; 164:93–100. [PubMed: 9795767]
6. Heeger PS, Lalli PN, Lin F, Valujskikh A, Liu J, Muqim N, Xu Y, Medof ME. Decay-accelerating factor modulates induction of T cell immunity. J Exp Med. 2005; 201:1523–1530. [PubMed: 15883171]
7. Medof ME, Kinoshita T, Nussenzweig V. Inhibition of complement activation on the surface of cells after incorporation of decay-accelerating factor (DAF) into their membranes. J Exp Med. 1984; 160:1558–1578. [PubMed: 6238120]
8. Wenderfer SE, Ke B, Hollmann TJ, Wetsel RA, Lan HY, Braun MC. C5a receptor deficiency attenuates T cell function and renal disease in MRLlpr mice. J Am Soc Nephrol. 2005; 16:3572–3582. [PubMed: 16207826]
9. Kumar V, Ali SR, Konrad S, Zwirner J, Verbeek JS, Schmidt RE, Gessner JE. Cell-derived anaphylatoxins as key mediators of antibody-dependent type II autoimmunity in mice. J Clin Invest. 2006; 116:512–520. [PubMed: 16453025]
10. Nataf S, Davoust N, Barnum SR. Kinetics of anaphylatoxin C5a receptor expression during experimental allergic encephalomyelitis. J Neuroimmunol. 1998; 91:147–155. [PubMed: 9846831]
11. Boos L, Campbell IL, Ames R, Wetsel RA, Barnum SR. Deletion of the complement anaphylatoxin C3a receptor attenuates, whereas ectopic expression of C3a in the brain exacerbates, experimental autoimmune encephalomyelitis. J Immunol. 2004; 173:4708–4714. [PubMed: 15383607]
12. Lin F, Fukuoka Y, Spicer A, Ohta R, Okada N, Harris CL, Emancipator SN, Medof ME. Tissue distribution of products of the mouse decay-accelerating factor (DAF) genes. Exploitation of a *Daf*1 knock-out mouse and site-specific monoclonal antibodies. Immunology. 2001; 104:215–225. [PubMed: 11683962]
13. Spicer AP, Seldin MF, Gendler SJ. Molecular cloning and chromosomal localization of the mouse decay-accelerating factor genes. Duplicated genes encode glycosylphosphatidylinositol-anchored and transmembrane forms. Journal of Immunology. 1995; 155:3079–3091.
14. Kerlero de Rosbo N, Mendel I, Ben-Nun A. Chronic relapsing experimental autoimmune encephalomyelitis with a delayed onset and an atypical clinical course, induced in PL/J mice by myelin oligodendrocyte glycoprotein (MOG)-derived peptide: preliminary analysis of MOG T cell epitopes. Eur J Immunol. 1995; 25:985–993. [PubMed: 7737302]
15. Tuohy VK, Lu ZJ, Sobel RA, Laursen RA, Lees MB. A synthetic peptide from myelin proteolipid protein induces experimental allergic encephalomyelitis. J Immunol. 1988; 141:1126–1130. [PubMed: 2456341]

NIH-PA Author Manuscript NIH-PA Author Manuscript NIH-PA Author Manuscript

16. Lin F, Fukuoka Y, Spicer A, Ohta R, Okada N, Harris CL, Emancipator SN, Medof ME. Tissue distribution of products of the mouse decay-accelerating factor (DAF) genes. Exploitation of a Daf1 knock-out mouse and site-specific monoclonal antibodies. Immunology. 2001; 104:215–225. [PubMed: 11683962]
17. Agresti A, Min Y. Unconditional small-sample confidence intervals for the odds ratio. Biostatistics. 2002; 3:379–386. [PubMed: 12933604]
18. Jabs C, Greve B, Chang TT, Sobel RA, Sharpe AH, Kuchroo VK. Genetic background determines the requirement for B7 costimulation in induction of autoimmunity. Eur J Immunol. 2002; 32:2687–2697. [PubMed: 12207354]
19. Bettelli E, Carrier Y, Gao W, Korn T, Strom TB, Oukka M, Weiner HL, Kuchroo VK. Reciprocal developmental pathways for the generation of pathogenic effector TH17 and regulatory T cells. Nature. 2006; 441:235–238. [PubMed: 16648838]
20. Furuzawa-Carballeda J, Vargas-Rojas MI, Cabral AR. Autoimmune inflammation from the Th17 perspective. Autoimmun Rev. 2007; 6:169–175. [PubMed: 17289553]
21. Hofstetter HH, Ibrahim SM, Koczan D, Kruse N, Weishaupt A, Toyka KV, Gold R. Therapeutic efficacy of IL-17 neutralization in murine experimental autoimmune encephalomyelitis. Cell Immunol. 2005; 237:123–130. [PubMed: 16386239]
22. Komiyama Y, Nakae S, Matsuki T, Nambu A, Ishigame H, Kakuta S, Sudo K, Iwakura Y. IL-17 plays an important role in the development of experimental autoimmune encephalomyelitis. J Immunol. 2006; 177:566–573. [PubMed: 16785554]
23. Lock C, Hermans G, Pedotti R, Brendolan A, Schadt E, Garren H, Langer-Gould A, Strober S, Cannella B, Allard J, Klonowski P, Austin A, Lad N, Kaminski N, Galli SJ, Oksenberg JR, Raine CS, Heller R, Steinman L. Gene-microarray analysis of multiple sclerosis lesions yields new targets validated in autoimmune encephalomyelitis. Nat Med. 2002; 8:500–508. [PubMed: 11984595]
24. Shenoy-Scaria AM, Timson Gauen LK, Kwong J, Shaw AS, Lublin DM. Palmitoylation of an amino-terminal cysteine motif of protein tyrosine kinases $p56^{lck}$ and $p59^{fyn}$ mediates interaction with glycosyl-phosphatidylinositol-anchored proteins. Molecular and Cellular Biology. 1993; 13:6385–6392. [PubMed: 8413237]
25. Shenoy-Scaria AM, Kwong J, Fujita T, Olszowy MW, Shaw AS, Lublin DM. Signal transduction through decay-accelerating factor. Interaction of glycosylphophatidylinositol anchor and protein tyrosine kinases $p56^{lck}$ and $p59^{fyn}$. Journal of Immunology. 1992; 149:3535–3541.
26. Bettelli E, Oukka M, Kuchroo VK. T(H)-17 cells in the circle of immunity and autoimmunity. Nat Immunol. 2007; 8:345–350. [PubMed: 17375096]
27. Harrington LE, Hatton RD, Mangan PR, Turner H, Murphy TL, Murphy KM, Weaver CT. Interleukin 17-producing CD4+ effector T cells develop via a lineage distinct from the T helper type 1 and 2 lineages. Nat Immunol. 2005; 6:1123–1132. [PubMed: 16200070]
28. Mangan PR, Harrington LE, O'Quinn DB, Helms WS, Bullard DC, Elson CO, Hatton RD, Wahl SM, Schoeb TR, Weaver CT. Transforming growth factor-beta induces development of the T(H)17 lineage. Nature. 2006; 441:231–234. [PubMed: 16648837]
29. Park H, Li Z, Yang XO, Chang SH, Nurieva R, Wang YH, Wang Y, Hood L, Zhu Z, Tian Q, Dong C. A distinct lineage of CD4 T cells regulates tissue inflammation by producing interleukin 17. Nat Immunol. 2005; 6:1133–1141. [PubMed: 16200068]
30. Veldhoen M, Hocking RJ, Atkins CJ, Locksley RM, Stockinger B. TGFbeta in the context of an inflammatory cytokine milieu supports de novo differentiation of IL-17- producing T cells. Immunity. 2006; 24:179–189. [PubMed: 16473830]
31. Weaver CT, Harrington LE, Mangan PR, Gavrieli M, Murphy KM. Th17: an effector CD4 T cell lineage with regulatory T cell ties. Immunity. 2006; 24:677–688. [PubMed: 16782025]
32. Lyons JA, S M, Happ MP, Cross AH. B cells are critical to induction of experimental allergic encephalomyelitis by protein but not by a short encephalitogenic peptide. Eur J Immunol. 1999; 29:3432–3439. [PubMed: 10556797]
33. Hjelmstrom P, J A, Fjell J, Ruddle NH. B-cell-deficient mice develop experimental allergic encephalomyelitis with demyelination after myelin oligodendrocyte glycoprotein sensitization. J Immunol. 1998; 161:4480–4483. [PubMed: 9794370]

NIH-PA Author Manuscript

NIH-PA Author Manuscript

NIH-PA Author Manuscript

34. Nataf S, Carroll SL, Wetsel RA, Szalai AJ, Barnum SR. Attenuation of experimental autoimmune demyelination in complement-deficient mice. J Immunol. 2000; 165:5867–5873. [PubMed: 11067947]

35. Esposito, A.; Suedekum, B.; Lin, F.; Lass, JH.; Medof, ME. Essential Roles of DAF and CD59 in Sustaining Successful Corneal Engraftment. Immunology 2004, International Proceedings, 12th International Congress of Immunology and 4th Annual Conference of FOCIS; Canada. 2004. p. 375-379.Publisher MEDIMOND S.r.l. Ed.Monduzzi, ISBN 88-7587-069-1

36. Gardinier MV, A P, Linington C, Matthieu JM. Myelin/oligodendrocyte glycoprotein is a unique member of the immunoglobulin superfamily. J Neurosci Res. 1992; 33:177–187. [PubMed: 1453482]

37. Sun J, L H, Olsson T, Xiao BG, Andersson G, Ekre HP, Linington C, Diener P. T and B cell responses to myelin oligodendrocyte glycoprotein in multiple sclerosis. J Immunol. 1991; 146:1490–1495. [PubMed: 1899688]

38. Killestein J, Polman CH. Current trials in multiple sclerosis: established evidence and future hopes. Curr Opin Neurol. 2005; 18:253–260. [PubMed: 15891408]

NIH-PA Author Manuscript
NIH-PA Author Manuscript
NIH-PA Author Manuscript

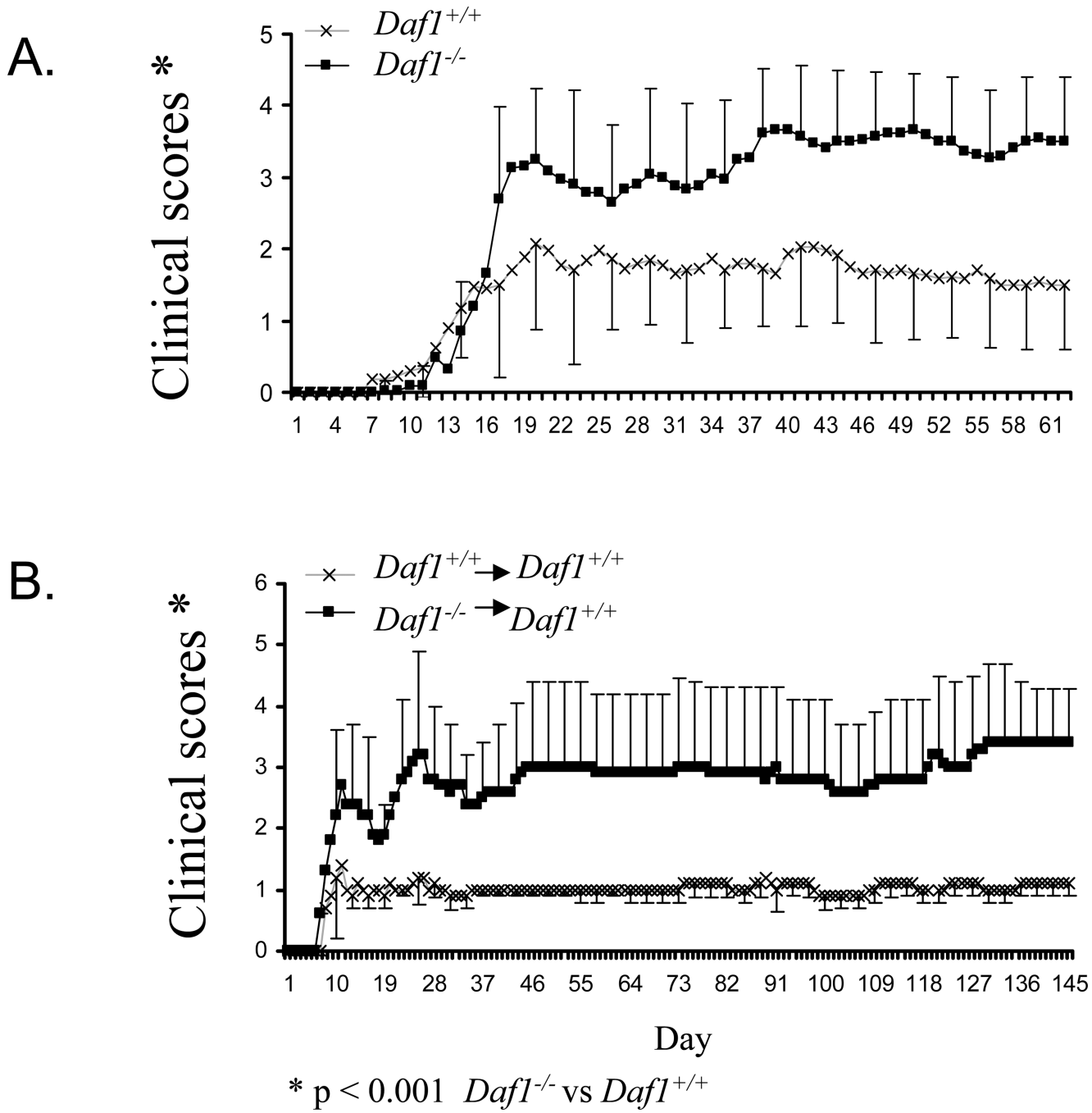

Figure 1. Clinical courses in $MOG_{35–55}$ immunized *Daf1*$^{-/-}$ and *Daf1*$^{+/+}$ mice

A) Clinical severity was scored daily in *Daf1*$^{-/-}$ mice (n=24) and *Daf1*$^{+/+}$ littermates (n=24). B) Clinical severity was scored daily in *Daf1*$^{+/+}$ recipients of adoptively transferred with spleen cells from *Daf1*$^{+/+}$ mice (n=5) and in *Daf1*$^{+/+}$ recipients of spleen cells from *Daf1*$^{-/-}$ mice (n=5). Data are an average from two independent experiments. *Daf1*$^{-/-}$ vs. *Daf1*$^{+/+}$ p<0.001.

NIH-PA Author Manuscript

NIH-PA Author Manuscript

NIH-PA Author Manuscript

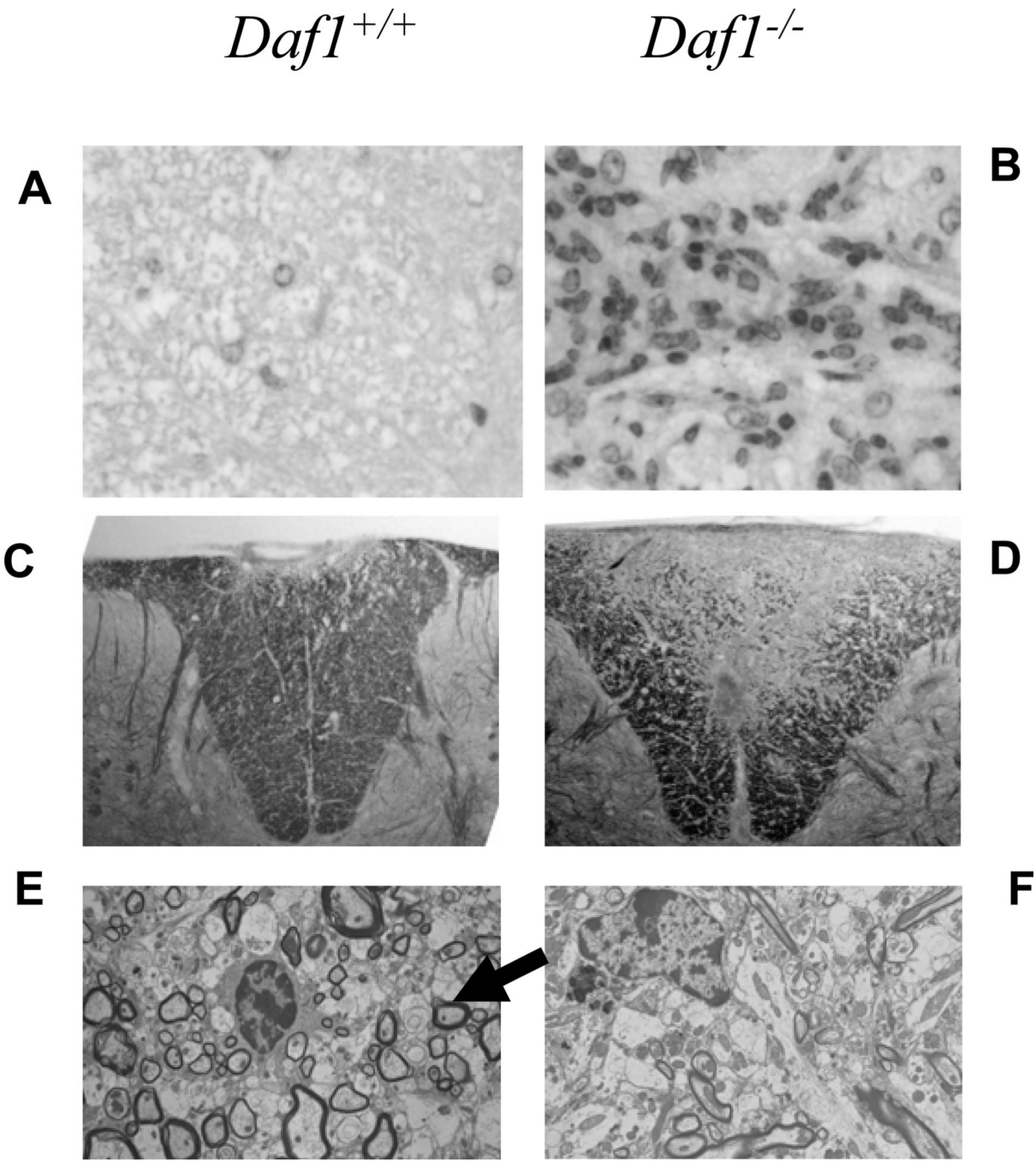

Figure 2. Neuropathology of spinal cords in $MOG_{35–55}$ immunized *Daf1*$^{-/-}$ and *Daf1*$^{+/+}$ mice

A and B) H&E staining of spinal dorsal column (magnification X100). C and D) Luxol fast Blue stains of dorsal column sections (magnification X100). E and F) Electron microscopy of lesions in dorsal columns at day 84 post immunization. E) The arrow shows thinly remyelinated axons in *Daf1*$^{+/+}$ mice.

NIH-PA Author Manuscript
NIH-PA Author Manuscript
NIH-PA Author Manuscript

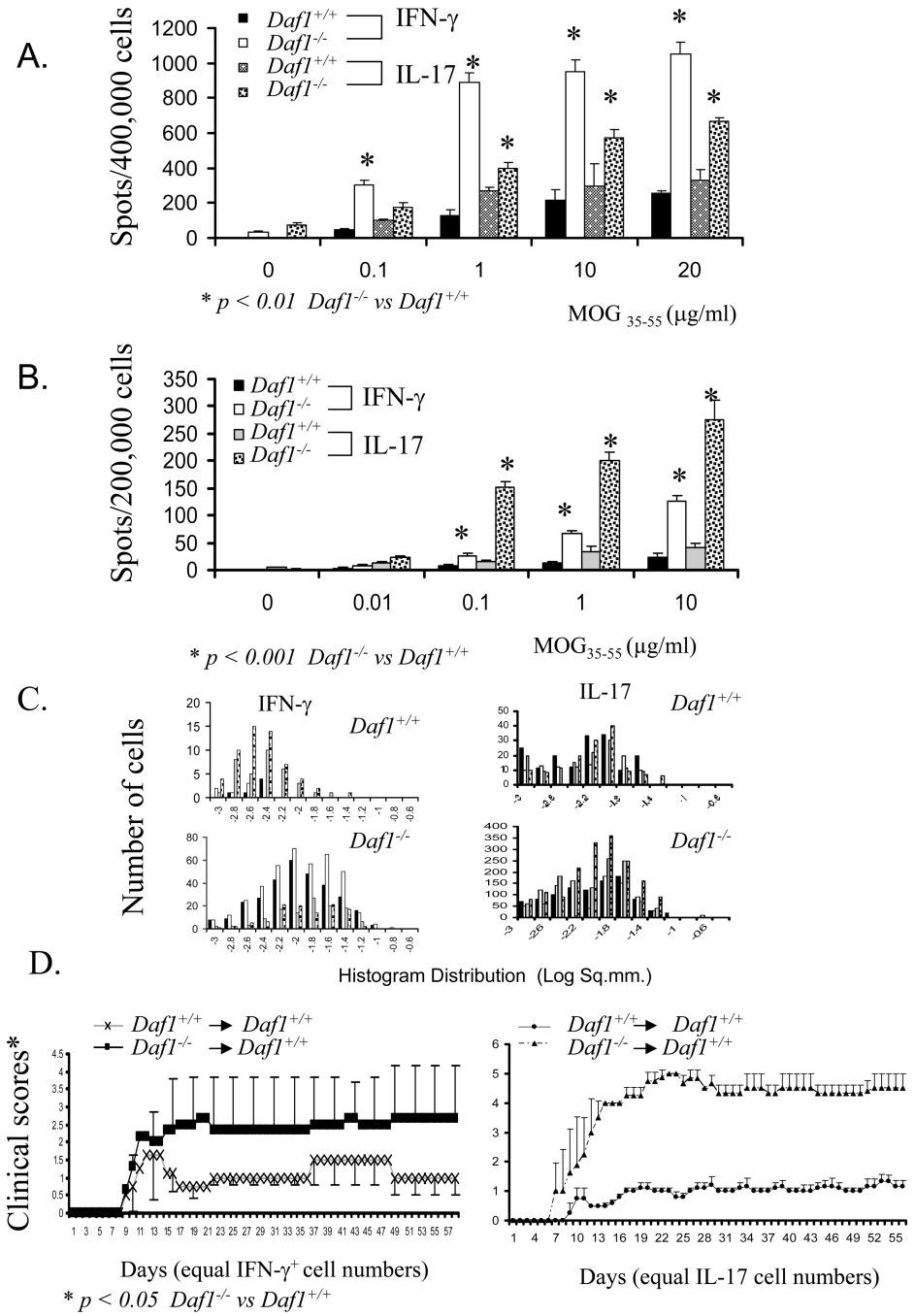

Figure 3.

T cell responses in $MOG_{35–55}$ immunized *Daf1*$^{-/-}$ and *Daf1*$^{+/+}$ mice to $MOG_{35–55}$ peptide and adoptive transfer of spleen cells from MOG immunized mice to naïve recipients

A) IFN-γ and IL-17 producing cells as assessed by ELISPOT assays at day 30 postimmunization. B) IFN-γ and IL-17 producing cells at day 60 post immunization. C) IFN-γ and IL-17 spot sizes in the presence of $MOG_{35–55}$. The data represent studies with 5 mice. The IFN-γ and IL-17 assays were done in the same spleens. The larger IFN-γ spot sizes of *Daf1*$^{-/-}$ T cells could be due to more IFN-γ or earlier onset of IFN-γ production (representative of 3 independent experiments at low spot density). D) Clinical scores of *Daf1*$^{+/+}$ recipients of the same numbers of adoptively transferred IFN-γ or IL-17 producing

NIH-PA Author Manuscript

NIH-PA Author Manuscript

NIH-PA Author Manuscript

spleen cells from $MOG_{35–55}$ immunized *Daf1*$^{-/-}$ and *Daf1*$^{+/+}$ mice. For these studies with equal numbers of IFN-γ or IL-17 producing cells, a portion of spleen cells was cultured with $MOG_{35–55}$ and 10 ng/ml IL-12 or 10 ng/ml of IL-23 for 72 hr, while another portion from the same spleen was incubated for 72 hr on ELISPOT plates to quantitate IFN-γ or IL-17 producing cells. Based on the IFN-γ ELISPOT counts following removal of adherent cells, 40×10^6 IL-12 treated spleen cells from *Daf1*$^{+/+}$ mice and 10×10^6 of the IL-12 treated spleen cells from *Daf1*$^{-/-}$ mice were transferred to *Daf1*$^{+/+}$ recipients. Based on the IL-17 ELISPOT, following removal of adherent cells 30×10^6 of IL-23 treated spleen cells from *Daf1*$^{+/+}$ mice and 10×10^6 of the IL-23 treated spleen cells from *Daf1*$^{-/-}$ mice were transferred to *Daf1*$^{+/+}$ recipients. The data represent 2 independent experiments.

NIH-PA Author Manuscript

NIH-PA Author Manuscript

NIH-PA Author Manuscript

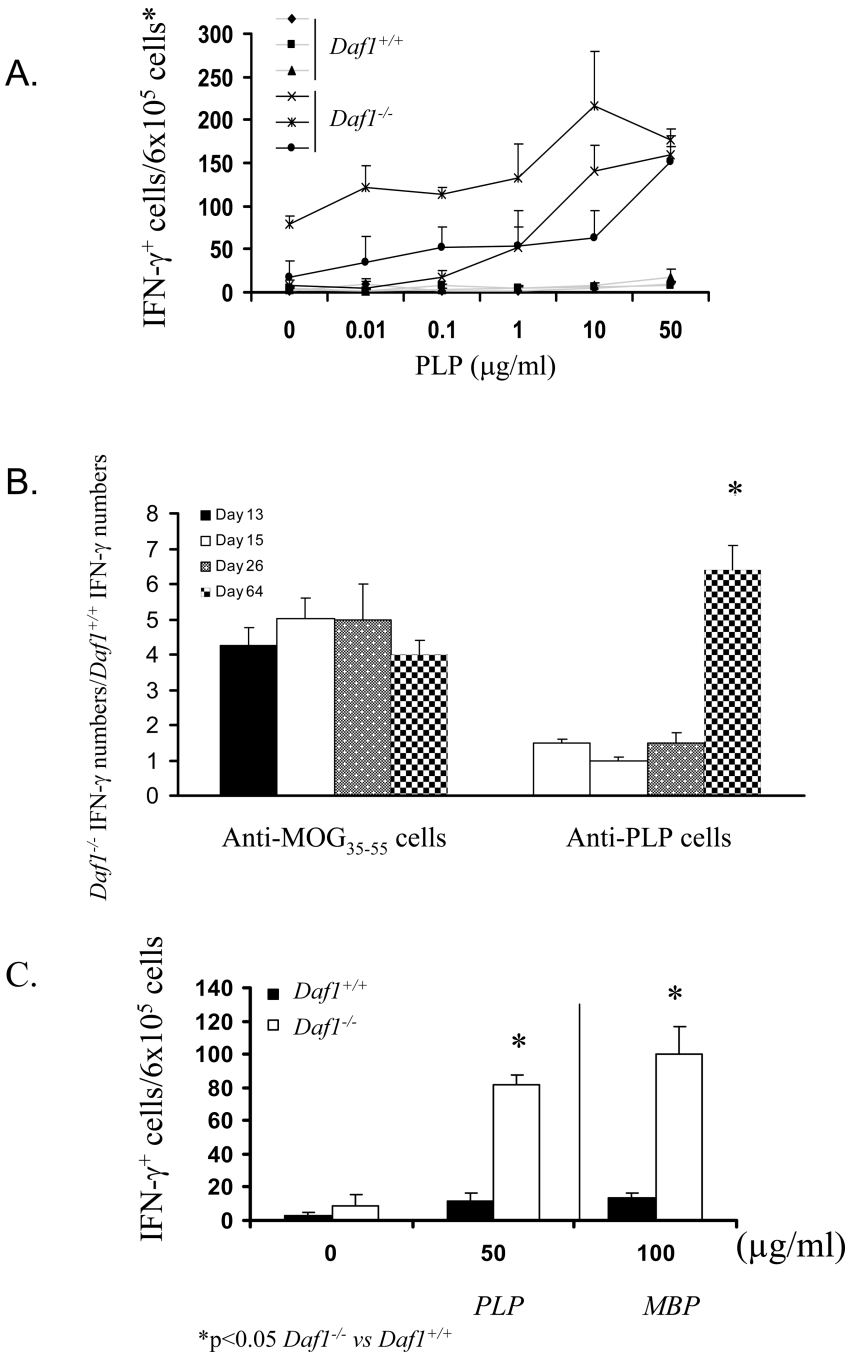

Figure 4. Epitope spreading to PLP and MBP in $MOG_{35–55}$ immunized *Daf1*$^{-/-}$ and *Daf1*$^{+/+}$ mice

A) IFN-γ responses to PLP protein of $MOG_{35–55}$ immunized *Daf1*$^{-/-}$ and *Daf1*$^{+/+}$ mice at day 56. In one *Daf1*$^{-/-}$ mouse, low reactivity with splenocytes (detectable in the absence of PLP probably representing spontaneous blastogenesis) did not differ in the presence of $Ova_{323–339}$ control. B) Kinetics of T cell responses of $MOG_{35–55}$ immunized mice spreading to PLP. Ratio of *Daf*$^{-/-}$ IFN-γ producing cells to *Daf1*$^{+/+}$ IFN-γ producing cells in response to the $MOG_{35–55}$ immunogen are shown on the left and spreading to PLP is shown on the right. C) IFN-γ recall responses in $MOG_{35–55}$ immunized mice at day 56 to PLP (50 μg/ml) and MBP (100 μg/ml).

NIH-PA Author Manuscript

NIH-PA Author Manuscript

NIH-PA Author Manuscript

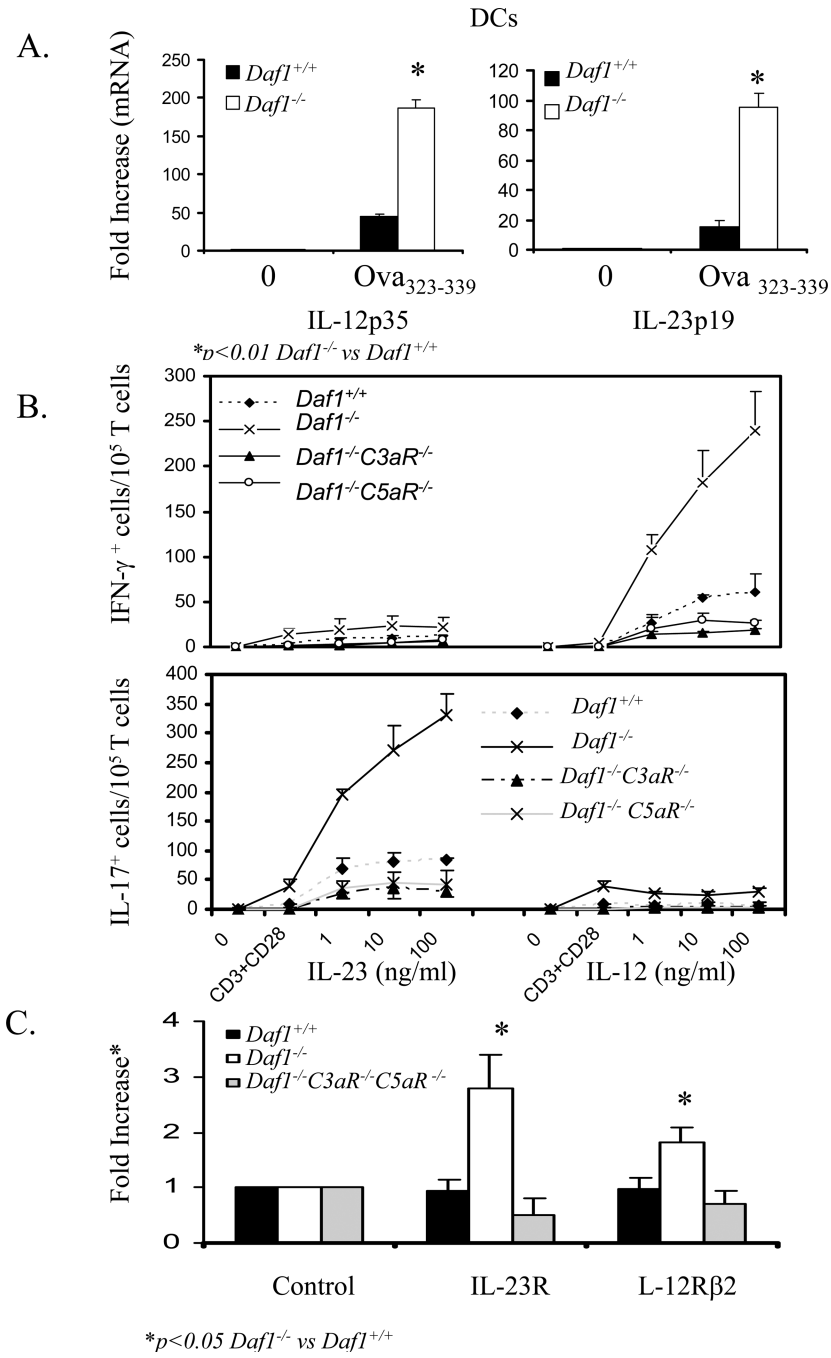

Figure 5. Effects of Daf deficiency and combined Daf•C5aR/C3aR deficiency on cytokine expression by APCs and cytokine receptor expression by T cells

A) IL-12p35 and IL-23p19 mRNA expression in flow separated DCs from *Daf1*$^{+/+}$ and *Daf1*$^{-/-}$ mice following 3 hr incubation with OT-II cells and ova$_{323–339}$. B) IFN-γ and IL-17 ELISPOT assays: T cells isolated by CD3^{+} T cell enrichment columns (R&D Systems) from *Daf1*$^{-/-}$ and *Daf1*$^{+/+}$ littermates were stimulated with anti-CD3 and anti-CD28 antibodies in the presence of increasing concentrations of IL-23 or IL-12. C) IL-23R and IL-12Rβ2 mRNA expression levels on T cells from *Daf1*$^{+/+}$, *Daf1*$^{-/-}$, and *Daf1*$^{-/-}$*C3aR*$^{-/-}$*C5aR*$^{-/-}$ mice stimulated with anti-CD3 and anti-CD28 antibodies.

NIH-PA Author Manuscript
NIH-PA Author Manuscript
NIH-PA Author Manuscript

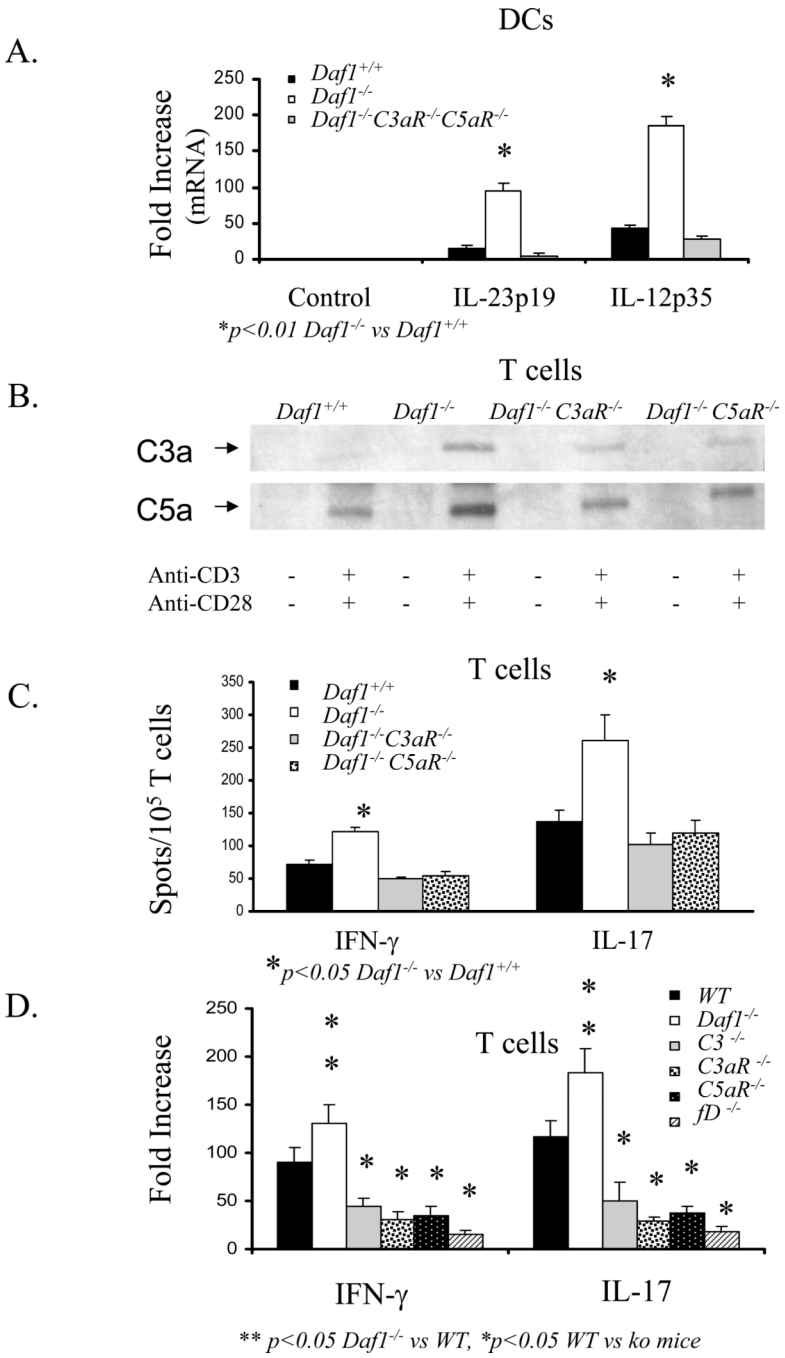

Figure 6. Augmented T cell responses by Daf deficient APCs and T cells depend on C5aR and C3aR

A) IL-23p19 and IL-12p35 mRNA expression in sorted *Daf1*$^{+/+}$, *Daf1*$^{-/-}$, and *Daf1*$^{-/-}$*C3aR*$^{-/-}$*C5aR*$^{-/-}$ DCs after incubation with ova$_{323–339}$ and OT-II cells. B). Western Blots of C3a and C5a in supernatants of *Daf1*$^{+/+}$, *Daf*$^{-/-}$, *Daf1*$^{-/-}$*C3aR*$^{-/-}$ and *Daf1*$^{-/-}$*C5aR*$^{-/-}$ T cells following anti-CD3 and anti-CD28 antibody stimulation. C) IFN-γ and IL-17 ELISPOT assays of *Daf1*$^{+/+}$, *Daf1*$^{-/-}$, *Daf1*$^{-/-}$ *C5aR*$^{-/-}$, and *Daf1*$^{-/-}$*C3aR*$^{-/-}$ T cells following anti-CD3 and anti-CD28 antibody stimulation. D) IFN-γ and IL-17 protein levels in supernatants of anti-CD3 and anti-CD28 antibody stimulated T cells from WT and

NIH-PA Author Manuscript

NIH-PA Author Manuscript

NIH-PA Author Manuscript

relevant knockout mice. T cell were isolated by $CD3^+$ T cell enrichment columns (R&D Systems).

NIH-PA Author Manuscript

NIH-PA Author Manuscript

NIH-PA Author Manuscript

A.

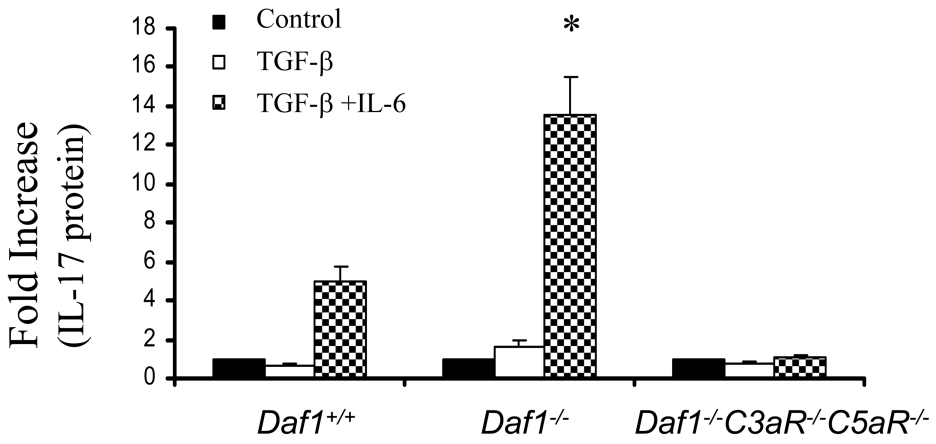

*P<0.01 Daf1 -/- vs. Daf1+/+

B.

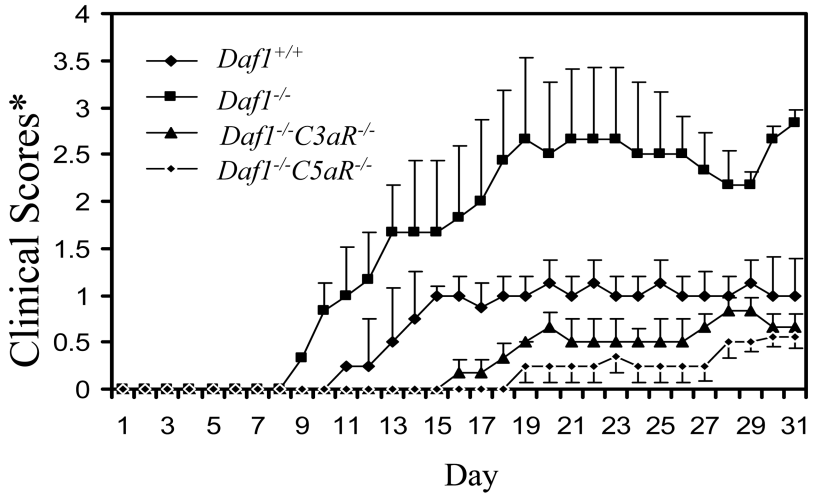

*P<0.01 Daf1 -/- vs. Daf1+/+, Daf1-/- C3aR-/- and Daf1-/-C5aR-/-

Figure 7. Differentiation of naïve CD4^{+}CD62L^{hi} T cells into IL-17 producing cells is augmented in the absence of Daf and markedly diminished in the absence of C5aR/C3aR and clinical scores are correspondingly decreased

A) Generation of IL-17 producing cells. Sorted naïve (CD4^{+} CD62L^{hi}) T cells were stimulated with anti-CD3 (5μg/ml), anti-CD28 (10 μg/ml), anti-IFN-γ (10 μg/ml), and anti-IL-4 (10 μg/ml) together with TGF-β or TGF-β plus IL-6 for 72 hr. Supernatants were assayed for IL-17 protein by the Beadlyte mouse multicytokine detection system. Naïve T cells treated with mAbs only served as a control. B) More severe EAE in *Daf1*$^{-/-}$ mice depends on C5aR and C3aR. Clinical scores of *Daf1*$^{-/-}$ (n=5) and *Daf1*$^{+/+}$ (n=5),

NIH-PA Author Manuscript

NIH-PA Author Manuscript

NIH-PA Author Manuscript

Daf1$^{-/-}$*C3aR*$^{-/-}$ (n=3), and *Daf1*$^{-/-}$*C5aR*$^{-/-}$ (n=3) mice measured daily after immunization with $MOG_{35–55}$.